Biomaterials 286 (2022) 121602

Contents lists available at ScienceDirect

Biomaterials

journal homepage: www.elsevier.com/locate/biomaterials

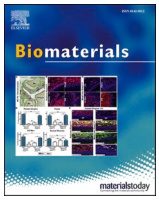

Production of food-grade microcarriers based on by-products from the food industry to facilitate the expansion of bovine skeletal muscle satellite cells for cultured meat production

R. Christel Andreassen [a], Sissel Beate Rønning [a], Nina Therese Solberg [a], Krister Gjestvang Grønlien [b], Kenneth Aase Kristoffersen [a], Vibeke Høst [a], Svein Olav Kolset [c], Mona Elisabeth Pedersen [a,*]

[a] Nofima AS, Raw Materials and Optimization, Ås, Norway
[b] Section for Pharmaceutics and Social Pharmacy, Department of Pharmacy, University of Oslo, Oslo, Norway
[c] Department of Nutrition, Institute of Basic Medical Sciences, University of Oslo, Oslo, Norway

ARTICLE INFO

Keywords:
Bovine skeletal muscle satellite cells (MuSCs)
Stem cell expansion
Cultured meat
Porous food-grade microcarriers (MCs)
By-products
Eggshell membrane (ESM)
Collagen
Biomaterials

ABSTRACT

A major challenge for successful cultured meat production is the requirement for large quantities of skeletal muscle satellite cells (MuSCs). Commercial microcarriers (MCs), such as Cytodex®1, enable extensive cell expansion by offering a large surface-to-volume ratio. However, the cell-dissociation step post cell expansion makes the cell expansion less efficient. A solution is using food-grade MCs made of sustainable raw materials that do not require a dissociation step and can be included in the final meat product. This study aimed to produce food-grade MCs from food industry by-products (i.e., turkey collagen and eggshell membrane) and testing their ability to expand bovine MuSCs in spinner flask systems for eight days. The MCs' physical properties were characterized, followed by analyzing the cell adhesion, growth, and metabolic activity. All MCs had an interconnected porous structure. Hybrid MCs composed of eggshell membrane and collagen increased the mechanical hardness and stabilized the buoyancy compared to pure collagen MCs. The MuSCs successively attached and covered the entire surface of all MCs while expressing high cell proliferation, metabolic activity, and low cell cytotoxicity. Cytodex®1 MCs were included in the study. Relative gene expression of skeletal muscle markers showed reduced PAX7 and increased MYF5, which together with augmented proliferation marker MKI67 indicated activated and proliferating MuSCs on all MCs. Furthermore, the expression pattern of cell adhesion receptors (ITGb5 and SDC4) and focal adhesion marker VCL varied between the distinct MCs, indicating different specific cell receptor interactions with the various biomaterials. Altogether, our results demonstrate that these biomaterials are promising prospects to produce custom-fabricated food-grade MCs intended to expand MuSCs.

1. Introduction

A novel food biotechnology alternative has emerged due to the increased demand for meat and the considerable environmental impact of the meat industry. In theory, cultured meat technology allows a significantly lower energy input with high protective ecological implications [1]. Cultured meat is based on growing skeletal muscle satellite cells (MuSCs) outside the living animal, where cells are isolated from a tissue biopsy and expanded in three-dimensional (3D) cell cultures such as bioreactor systems using microcarriers (MCs) [2]. Therefore, a sustainable food-grade MC adapted for optimal MuSC proliferation to ensure high-density cell culture is among the prerequisites to facilitate cultured meat production. The standard technique for growing adherent cells (e.g., MuSCs) is in single-cell monolayers on flat rigid surfaces [3]. Monolayer cell growth results in a small surface to volume ratio, limiting the production potential. One promising option for cultured meat production is to expand isolated cells on the surface of small, solid, and often spherical materials such as MCs in a bioreactor. Cells expanded in a MC-based bioreactor system benefit from a significantly larger surface area to volume ratio compared to monolayered cultures. MCs are typically 100–500 μm in diameter and differ in their physical properties such as porosity, density, size, rigidity, and surface chemistry [4,5].

* Corresponding author. Osloveien 1, 1433, AAS, Norway.
E-mail address: mona.pedersen@nofima.no (M.E. Pedersen).

https://doi.org/10.1016/j.biomaterials.2022.121602
Received 11 November 2021; Received in revised form 11 May 2022; Accepted 23 May 2022
Available online 27 May 2022

Commercially available MCs are often made with materials such as glass, diethyl aminoethyl (DEAE)-dextran, polyacrylamide, polystyrene, and cellulose [5,6]. These MCs generally need surface treatments such as texturizing, a coating of extracellular matrix (ECM) proteins, or at the most basic level, an ionic charge to attract cells and promote cell adherence [4,5]. They also require a cell MC dissociation step following cell expansion. While the dissociation process varies (e.g., chemical, or mechanical), it often results in a significant cell/tissue yield loss due to incomplete cell detachment or MC aggregation [7,8]. This makes cultured meat production less efficient and more costly. While natural and synthetic collagen is already commonly used in tissue engineering for scaffold production, it is to our best knowledge not specifically developed for food production applications or agitated cell culture systems. They usually lack the structural stability needed in agitated cell culture and are often expensive polymers [8]. The commercially available MCs adapted for genetically stable cell lines used in the medical field are not acceptable food-grade. However, at present exciting work is currently ongoing on food-grade scaffold production using textured soy protein and salmon gelatin [9,10]. This work focuses on the feasibility of using by-products to develop food-grade MCs that will not require a dissociation step by being included in the final cultured meat product. This can reduce profit loss by ensuring high cell expansion with maximum recovery of bovine MuSCs.

The optimal biomaterial to use in the design of MCs for cultured meat production should be capable of mimicking the natural 3D network that provides structural support and maintains normal cellular behavior in MuSCs, i.e., the ECM [11,12]. As cultured meat provides the opportunity to customize the nutritional composition of the food product, it is beneficial to produce MCs with nutrient-enhancing components that can be included in the final meat product. Hence it would be ideal to use food-grade biocompatible materials with naturally high cell-stimulating properties, combined with previous knowledge of MC dynamics. By-products from the food industry such as poultry carcasses and eggshell membranes (ESM) are excellent sources for collagen, glycoproteins, and proteoglycans that are all present in the ECM. The availability of poultry by-products will also increase over the coming decade as poultry meat production is expected to account for 52% of the global growth in meat production [13]. By-products are low-cost, easy to obtain, and food-safe ingredients with high nutritional value [14]. Further, the processing of poultry by-products by enzymatic protein hydrolysis have shown that collagen-rich products can be extracted from mixed side stream materials, such as turkey carcasses [15]. Nearly 30% of the eggs consumed globally by humans are broken and processed or powdered into foods. Norway's leading producer of egg products, Nortura Eggprodukter AS, produces about 800 tons of egg waste (i.e. 40 tons ESM and 760 tons ES), forming a solid basis for Norwegian industrial development and possibility to increase the profit of waste. Use of ESM as food ingredient has been calculated to increase the value up to 10 USD/kg communicated. The Norwegian biotechnology company Biovotec AS has developed a unique separation technology for egg waste (WO 2015058790 A1) which is implemented in a one-of-a-kind plant developed by Nortura Eggprodukter AS. This plant provides egg waste material for improved industrial exploitation. Most importantly, using by-products will aid resource recycling and give significant value to by-products that otherwise would be an environmental burden by their destruction methods.

Collagen materials from poultry sources were particularly interesting in this study due to their high mechanical strength under the stressful conditions in agitated cell cultures. This is because avian collagen demonstrates among the highest denaturation temperatures reported in nature [16,17]. ESM has a high collagen content in addition to a high density of disulfide bridges which increases its mechanical strength [18]. Previous work in our laboratory has shown that processed ESM powder is highly bioactive, anti-inflammatory, regulates cellular functions during wound healing, and is a promising biomaterial for tissue engineering [19–22]. It has also been demonstrated that combining collagen with ESM and crosslinking the scaffold with dehydrothermal (DHT) treatment improved the mechanical properties of collagen [21,22]. However, this treatment is not suitable for food applications due to the high toxicity [23]. Therefore, in this study, we selected collagen extracted from turkey-tendons, ESM and a non-toxic UVA-riboflavin crosslinking method to produce food-grade MCs. This study aimed to develop three unique types of MCs and investigate their suitability in agitated cell culture. The MCs physical properties were characterized and monitored for their cell growth-promoting potential in spinner flasks with bovine MuSCs expanded for eight days. Commercially available Cytodex®1 MCs were tested in the same culture system for comparison. To the best of our knowledge, this is the first report on MCs produced with low-cost food by-product materials that are assessed in agitated cell culture.

2. Materials and methods

2.1. Raw materials and chemicals

Raw material by-products from turkey and eggshell membrane (NOR-ESM) were provided by Norilia (Oslo, Norway). Dulbecco's Modified Eagle Medium (DMEM) low glucose supplemented with GlutaMAX™ and pyruvate, fetal bovine serum (FBS) and penicillin/streptomycin solution 10 000 units per mL (P/S), Amphotericin B, and 0.05% trypsin/EDTA were purchased from Thermo Fisher Scientific (Waltham, MA, USA). Entactin-Collagen-Laminin (ECL) was purchased from Millipore Sigma (Burlington, MA, USA). Collagenase and Cytodex®1 MCs were Sigma Aldrich (Merck KGaA, Darmstadt, Germany). Unless otherwise stated, all other reagents were from Sigma Chemicals Co. (St. Lois, MO, USA). Collagen was extracted from turkey tendons as described by Grønlien et al. [16]. In short, turkey tendons were dissected from slaughterhouse by-product material and extracted for collagen using pepsin in acetic acid and precipitated in 4 M NaCl. The solution was dialyzed (Spectra/Por Dialyzer tubing, MW cutoff 12 000 kDa, Cat. No 3787-D42 tubing, Thomas Scientific, MJ, US) and freeze-dried. Eggshell membrane (NOR-ESM) was harvested using a patented process by Biovotec AS (WO 2015058790 A1) and washed with 0.1 M hydrochloric acid (HCl) for 10 min under 300 rpm stirring, then washed twice with dH_2O before it was freeze-dried at 0.0019 mbar for 72 h (Martin CHRIST, Gamma 1–16 LSCplus, Osterode am Harz, Germany) and milled (ZM 200 Ultra centrifugal mill, Retsch, Haan, Germany) to a powder with an average particle size of 0.25 mm.

2.2. Production and characterization of food-grade MCs (Collagen, hybrid, and ESM)

2.2.1. Preparation of MCs

The collagen MCs were produced by dissolving collagen isolated from turkey tendons in 20 mM acetic acid (10 mg/mL) under 300 rpm stirring. To create spheres, the solution was dripped into liquid nitrogen with a quince tip syringe (21.5G). The same procedure was repeated to produce the hybrid MCs consisting of a 1:1 mixture of turkey tendon collagen and ESM. After liquid nitrogen evaporation at room temperature, the MCs were freeze-dried at 0.0019 mbar for 48 h (Martin CHRIST, Gamma 1–16 LSCplus, Osterode am Harz, Germany) and kept at 4 °C until further use. The ESM MCs was prepared by shifting the ESM powder using a laboratory sieve shaker (AS 300 Control, Reusch, Haan, Germany) with a stack of sieves with pore sizes 100 and 200 μm (Reusch, Haan, Germany). The isolated fraction was analyzed with a Helium–Neon Laser Optical System (Sympatic Inc., Clausthal-Zellerfeld, Germany). Cytodex®1 MCs were prepared according to the manufacturer's instructions. In short, 114 mg MCs were transferred to borosilicate bottles with polypropylene caps and set to swell for 3.5 h in 100 mL phosphate buffered saline (PBS). The MCs were washed with PBS before autoclaving at 121 °C (15 min) and washed again with PBS. They were then transferred to spinner flasks with cell culture media.

The crosslinked collagen and hybrid MCs were prepared by soaking 50 mg collagen and 100 mg hybrid MCs in 10 mL of a 0.1% (w/v) solution of riboflavin 5′-monophosphate sodium salt (Sigma-Aldrich, Saint Louis, MO, USA) in 70% EtOH subjected to UVA irradiation from three fluorescent tubes (Ralutec 9W/78, Radium, Germany; $\lambda_{max} = 365$ nm, 2.94 mW/cm^2) in a chamber (Polylux-PT, Dreve, Germany) for 5 min, then washed with PBS three times to remove residual riboflavin and sterilized in 70% EtOH for 10 min. The MCs were washed another time with PBS before transferring to spinner flasks with culture media. 50 mg ESM powder was sterilized in 70% ethanol for 10 min, then washed with PBS and stored at 4 °C before use or transferred directly to cell culture media in spinner flasks.

2.2.2. Measurements of physical properties

The average size of swollen collagen and hybrid MCs was calculated by employing the ZEISS Axio software tool measuring their diameter from 20 to 22 randomly selected pictures captured with the ZEISS Axio Observer Z1 microscope. The average particle size of ESM powder was measured using a Helium–Neon Laser Optical System according to the manufacturer's instructions. The mechanical properties (force, N and Young's modulus, Pa) of the derived collagen and hybrid MCs were studied using TA-XTplusC Texture Analyzer (Stable Micro Systems, Haslemere, UK) in compression mode. The MCs were prepared as described in the preparation of MCs procedure (2.2.1). The resulting MCs were rinsed with PBS and exposed to constant pressure at 0.01 mm/s with a maximum strain set to 50% by a cylindrical probe (ø = 6 mm) attached to a 500 g load cell. The probe was positioned approximately 1 mm above the sample before analysis. The Young's moduli for the MCs were defined as the slope of the linear central portion of the stress-strain curve between 15 and 25% strain. Swelling capacities (SC) of ESM, collagen and hybrid MCs were measured over time (1, 24, 72, 144 and 192 h) in PBS (pH 7.4) at room temperature. The dry materials were weighed (W_1) and soaked in PBS, then the PBS was removed, and the wet materials (W_2) were weighed again. Each sample was measured in three individual replicates and the average values were used to calculate SC with the following equation:

$$SC = \frac{W_2 - W_1}{W_1} \quad (1)$$

2.2.3. Scanning electron microscopy of MCs

All samples were dehydrated in 100% ethanol (EtOH) and dried using a Critical Point Dryer (CPD 030, Bal-tec AG, Schalksmühle, Germany) with liquid carbon dioxide as the transitional fluid. Then the samples were mounted on aluminum stubs with double-sided carbon tape and coated with gold-palladium (Polaron Emitech SC7640 Sputter Coater, Quorum technologies, East Sussex, United Kingdom) and examined by Environmental Scanning Electron Microscope (EVO® 50 Series, Carl Zeiss AG, Oberkochen, Germany). The imaging was performed at the Imaging Centre, Faculty of Biosciences, Norwegian University of Life Sciences.

2.2.4. 2,4,6-trinitrobenzenesulfonic acid (TNBS) assay of MCs

The content of primary amines in the MCs was determined using a modified TNBS assay [24,25]. The TNBS assay is one of several methods used to quantify primary amines in protein samples. This method is typically used to determine the amount of cleaved peptide bonds after proteolytic reactions (i.e., degree of hydrolysis) or to measure reduction in primary amines due to for example crosslinking reactions where primary amines are the target [24]. A calibration curve with a concentration rage from 0 to 0.05 mg/mL glycine was prepared from a 5 mg/mL stock solution diluted in 4% (w/v) $NaHCO_3$. 0.70–0.80 mg samples were hydrated with 0.25 mL 4% (w/v) $NaHCO_3$ overnight at room temperature in 2 mL Eppendorf tubes. The standards were prepared by transferring 0.25 mL standard solution to 2 mL Eppendorf tubes. 0.25 mL freshly prepared 0.05% (w/v) TNBS solution was added to the samples and standard solutions. The samples and standards were incubated at 40 °C for 2 h before addition of 0.75 mL 6 M HCl. After the addition of HCl the samples were incubated at 60 °C for 90 min to dissolve the sample materials. Following the acid treatment, the samples were cooled to room temperature and centrifuged for 30 s using a benchtop centrifuge from Labnet International (Edison, NJ, USA). 50 μL of the sample solutions and standards were transferred to a Pierce 96-Well Polystyrene Plate (Thermo Fisher Scientific, Waltham, MA, USA) and diluted with 50 μL Milli-Q water per well. Absorbance was measured at 320 nm using a Synergy H1 Hybrid Multi-Mode Microplate Reader (Biotek, Bad Friedrichshall, Germany). All samples were measured against blanks which were prepared as described above except the 6 M HCl was added prior to the addition of TNBS. The samples, blanks and calibration solutions were measured in triplicates. Primary amines (mmol/g sample) were calculated from the standard curve and the percent reduction in primary amines was calculated relative to untreated MCs.

2.2.5. Pore size

Pore size distribution was measured by mercury intrusion porosimetry using a Micromeritics AutoPore IV 9500 (Micromeritics Instrument Corporation, Norcross, GA, USA). A powder-type penetrometer (Model #14) with a stem volume of 0.4120 mL and a penetrometer volume of 3.1188 mL was used. The pressure range investigated was 0.10–60000 psia.

2.3. Cell culture experiments on MCs

2.3.1. Bovine skeletal muscle satellite cell (MuSC) isolation

Bovine MuSCs were isolated from freshly slaughtered beef sirloin provided by Nortura AS (Rudshøgda, Norway) using an established protocol [26,27]. In short, a muscle biopsy of ~2 g was digested with 0.72 mg/mL collagenase in 10 mL DMEM containing 10.000 units/mL penicillin/streptomycin (P/S) and 250 μg/mL amphotericin B for 1 h at 37 °C with 70 rpm shaking. The tissue was further digested with 0.05% trypsin/EDTA (25 min) before adding 10% FBS for enzyme inactivation, and this step was repeated three times before the cell pellets were pooled together. To purify MuSCs and remove fibroblasts, the cell pellets were incubated in uncoated 25 cm^2 culture flasks for 1 h at 37 °C and 5% CO_2 in culture seeding medium (DMEM) supplemented with 10% fetal bovine serum (FBS), 250 μg/mL fungizone, and 10.000 units/mL P/S. Fibroblasts adhere to the plastic and the non-adhering MuSCs were collected and transferred to cell flasks coated with 1 mg/mL Entactin-Collagen-Laminin (ECL). When the cells reached 70–80% confluence, they were harvested in freezing media (8% dimethyl sulfoxide in DMEM media) and stored in liquid nitrogen.

2.3.2. Spinner flask cell culture

The starting cell culture with isolated MuSCs was passaged in 175 cm^2 cell culture flask in cell growth medium containing DMEM medium supplemented with 2% FBS, 2% Ultroser G, 250 μg/mL fungizone, and 10.000 units/mL P/S. When confluency of ~80% was reached, the cells (~1 million cells) were inoculated into 250 mL spinner flasks (Bellco Glass, NJ, USA) mixing the cells with 10 mL cell growth medium and MCs. The spinner flasks were placed in a humified incubator at 37 °C and 5% CO_2 with no agitation for approximately 13 h to allow cell attachment. The growth medium was then adjusted to 100 mL and the spinner flasks were placed on a magnetic stirrer at 100 rpm. Three replicate spinner flasks were performed for each different MC type, and samples were taken on days 1, 3, 6 and 8.

2.3.3. Cell proliferation, metabolic activity, and cytotoxicity assay

Cell proliferation was measured as the amount of dsDNA using a Quant-IT Picogreen dsDNA Assay (Fluorescence) (Invitrogen, Paisley, UK) according to the manufacturer's instructions. Prior to analysis, the samples were washed with PBS and the pellet was lysed with 150 mL

RLT buffer (Qiagen GmbH, Venlo, Netherlands). The solution was incubated at 55 °C for 15 min, vortexed and stored at −80 °C until further use. Cell metabolic activity was measured as ATP using CellTiter-Glo ®Luminescent assay (Promega, Madison, WI, USA). Muscle cell cytotoxicity was measured as lactate dehydrogenase (LDH) release in the media, using a Cytotoxicity Detection Kit (Roche Applied Science, Mannheim, Germany) according to manufacturer's instructions. Luminescent and absorbance, respectively, were measured using a Synergy H1 Hybrid multi-mode microplate reader (Biotek, Winooski, VT, USA). The samples were performed in triplicates, and data are presented as mean ± SD.

2.3.4. Glucose consumption and lactic acid production

Glucose and lactic acid concentrations were measured using the Reflectoquant test with corresponding test strips and RQflex 10 instrument (Merck KGaA, Darmstadt, Germany) following the manufacturer's instructions. The method to measure glucose is based on the conversion of glucose into gluconic acid lactone. The hydrogen peroxide formed reacts with an organic redox indicator to form a blue-green dye. The method to measure lactic acid is based on the oxidation of lactate by nicotinamide adenine dinucleotide (NAD) and lactate dehydrogenase to pyruvate. When NADH is produced it reduces tetrazolium salt to a blue formazan. The samples were performed in duplicates from the individual spinner flask, and data are presented as mean ± SD.

2.3.5. Immunocytochemistry and light microscopy

The cell nuclei were visualized using a Hoechst stain (Invitrogen, NucBlue, Live Cell Stain ready probe, Hoechst 33342). The cell growth medium was removed, and the samples were washed once in PBS and resuspended in 500 μL PBS. The stain was added per the manufacturer's instruction (1 drop/500 μL) and incubated dark at room temperature for 20 min. The MuSC/MC suspension was transferred onto a microscope slide and examined by fluorescence microscopy analysis. During immunofluorescence staining, the samples were washed with PBS and fixed with 4% PFA for 10 min at room temperature. The samples were then washed once with PBS and permeabilized with 0.1% Triton-X-100 for 15 min. Samples were blocked in 1X blocking buffer (ab126587) in PBS-tween (PBS-t) for 30 min, followed by incubation with the primary antibody for 60 min at room temperature. The samples were washed twice with PBS and incubated with secondary antibody, Alexa Fluor™ 488 Phalloidin probe (1:200) and NucBlue Live Cell Stain ready probe for 1 h and washed once with PBS before the samples were transferred onto a microscope slide and mounted using the DAKO fluorescent mounting medium (Glostrup, Denmark). The antibodies used were mouse anti α-Tubulin T5168 1:400 (Sigma Aldrich), Alexa 488-conjugated goat anti-mouse and Alexa 546-conjugated goat anti-mouse (Thermo Fisher Scientific, Waltham, MA, USA) 1:400. Mouse anti-NCAM/CD56 5.1H11, 1:10 was from Developmental Studies Hybridoma Bank (Iowa city, IA, USA). Primary and secondary antibodies were diluted in 0.1X blocking buffer in PBS-t. All images were produced with a ZEISS Axio Observer Z1 microscope and images were processed using Adobe Photoshop CS3. When necessary, adjustment in brightness and contrast were performed across the entire image.

2.3.6. RNA extraction and real-time quantitative PCR (RT-qPCR)

Total RNA was isolated using the RNeasy MiniKit (Qiagen, cat#74104) according to the manufacturer's instructions. First, MuSC/MC samples were centrifuged (300 g) for 5 min and washed once with PBS and before the cells were lysed with 350 mL RLT buffer containing 2 M DTT. cDNA was generated from ~2 to 10 ng total RNA using TaqMan®Reverse Supersripct ViLO (Invitrogen, Carlsbad, CA) according to the manufacturer's protocol. Real-time qPCR analysis was carried out using a TaqMan Gene expression Master Mix (Life Technologies) and QuantStudio5 (Applied Biosystems, Foster City, CA, USA) PCR System. The amplification protocol was initiated at 50 °C for 2 min, followed by denaturation at 95 °C for 10 min, then 45 cycles of denaturation at 95 °C for 15 s, annealing of TaqMan probes and amplification at 60 °C for 1 min. RT-qPCR analyses were performed on 1 biological replicate, with 3 technical replicates. The ΔCt values were calculated according to the MIQE guidelines and the relative gene expression (fold change) was calculated by formula $2^{-\Delta\Delta Ct}$ [28,29]. The relative gene expressions were normalized to the *EEF1A1* internal control, and the bars indicate fold change relative to mean of the Day 0 control sample for each gene analyzed. All TaqMan® primer/probes are listed in Table 1.

2.4. Data treatment

Each spinner flask experiment was carried out in triplicates and repeated in at least three individual biological replicates. The sample analysis was performed in triplicates from samples of each individual spinner flask unless otherwise stated, and data were presented as mean ± SD. Significant variance was determined by one-way ANOVA using Dunnett's multiple comparison test. Differences were considered significant at $p < 0.05$. All statistical analysis was performed in Graph Pad Prism version 7.04 (GraphPad Software, La Jolla, CA, USA).

3. Results and discussion

3.1. Production and characterization of food-grade MCs

Three different MCs, *i.e.*, collagen, a "hybrid" consisting of a 1:1 mixture of collagen and ESM, and ESM MCs, were produced using food-grade collagen extracted from turkey tendons and ESM powder. The collagen-based MCs were also crosslinked using UVA-riboflavin to increase their mechanical strength. UVA-riboflavin is a non-toxic alternative to other surface treatment options such as glutaraldehyde (GA)- and dehydrothermal (DHT) crosslinking. Texture analysis, swelling tests, size measurements, primary amines, and scanning electron microscope (SEM) analysis were preformed to investigate the physicochemical properties of the MCs.

The food-grade raw materials used to produce the MCs have different compositions and structures which can be exploited to produce MCs with different properties. Collagen from turkey tendons is partly hydrolyzed because of the extraction process and consist mainly of collagen I and III [16]. Collagens I and III have the typical triple helical structure composed of three polypeptide chains. The amino acid composition of collagen is also characteristic, every third amino acid is glycine and the remaining positions in the chain are mainly filled by the amino acids: proline and hydroxyproline [30]. Elevated hydroxyproline content is associated with higher thermostability. The hydroxyproline contented in collagen from warm-blooded animals is therefore higher compared to the collagen from coldblooded animals. Collagen from turkeys, which have a body temperature around 40 °C, has one of the highest registered denaturation temperatures [16]. The ESM is a meshwork of fibers naturally stabilized by extensive crosslinking and mainly consists of structural proteins such as collagen (III and V). In addition to high amounts of collagen proteins, the ESM also contains cysteine-rich eggshell membrane proteins (CREMPs) [18]. CREMPs have molecular disulfide linkages within the cysteine-rich repeat domains giving the ESM increased mechanical strength in the wall of nematocysts to help withstand extreme osmotic pressure [31,32]. Both raw materials

Table 1
Gene target and TaqMan®primer/probe assays.

Gene target	TaqMan®primer/probe assays
EEF1A1	Bt03223794_gl
PAX7	Hs00242962_ml
MYOD1	Bt03244740_ml
SDC4	Mm01179833_m1
ITGB5	Bt03223516_m1
VCL	Bt03217637_g1
MKI67	Hs04260396_g1

have excellent properties for use in cell culturing. However, producing MCs with one or a combination of the two biomaterials for MuSC culture to withstand temperatures of 37 °C and the mechanical stress under agitation have not yet been investigated. The focus in this study was therefore to produce prototype MCs based on turkey collagen and ESM for efficient MuSC expansion. UVA-riboflavin crosslinking was used to increase the stability of the MCs. The UVA-riboflavin treatment leads to oxidation of amino acid side groups and covalent bonds by a photochemical reaction involving the formation of reactive oxygen species (ROS) and singlet oxygen ($^1O_2$). Crosslinking collagen with the use of UVA and riboflavin is well-known and it involves the formation of covalent bonds between the amino acid side chains of histidine, hydroxyproline, hydroxylysine, tyrosine, and threonine [23,24,30,33,34]. Crosslinking promotes the construction of more resilient and insoluble biomaterials. The results from the UVA-riboflavin primary amine analysis showed a reduction of 7.4% in the collagen and 24.2% in the hybrid MCs. This indicates an increase in crosslinking density for both MCs (Fig. 1A) even though the primary amine is not the only group participating in UVA-riboflavin induced crosslinking [34]. The UVA-riboflavin treatment increased mechanical hardness and elasticity for both MCs, and the effect was more pronounced in the hybrid MCs (Fig. 1B and C). Our initial preparations of hybrid beads included different ratios of collagen and ESM; however, the MCs were not stable (data not shown). For example, MCs were developed using 75% ESM and the beads dissolved within 2 h. The ratio of ESM and collagen in the hybrid MCs is largely determined by the ability of collagen to bind the ESM particles together, forming a more stable framework for the MCs. This work is "proof-of-concept" for using by-product biomaterials to produce MCs with efficient cell expansion, and no other ratios were tested for cell expansion.

The hybrid MC showed a lower capacity to absorb PBS than pure collagen, and both collagen-based MCs swelled more over time compared to ESM MCs (Table 2). The swelling capacity of ESM was lower with minor changes over time, supporting the high stability of this material. Interestingly, in previous work, where ESM was combined with bovine type 1 collagen and the DHT crosslinking method was applied, a significant increase in PBS absorption was observed [21]. It is unknown whether this was due to the differences in physical characteristics of turkey collagen used to generate MCs and bovine collagen type I used in the previous study, or whether the observed differences were due to the different crosslinking of the material. Previous work in our lab has shown that turkey collagen contains high purity collagen type I and III, and that the material retained the native triple helix after isolation. Likewise, this material is shown to have high thermal stability [16]. After three days, we observed a loss in swelling capacity for collagen-based MCs, which may be due to an internal collagen collapse upon rehydration as only the surface of the MCs may be crosslinked. To further strengthen the collagen structure internally, the riboflavin mixture can be included in the initial solution and crosslinked before producing spherical MCs in further studies. Texture and water binding properties of a final cultured meat product is a highly important quality parameter for consumers preference. These food-grade MCs can be included in the final meat product and would therefore influence these parameters. ESM has high mechanical properties and could positively add to more meat-like texture properties.

Table 2
Swelling capacity (SC) timeseries of MCs.

Time	1 h	1 day	3 days	6 days	8 days
Collagen MCs	12.98 ± 3.68	16.00 ± 2.24	19.45 ± 3.83	14.92 ± 1.4	14.02 ± 0.79
Hybrid MCs	10.49 ± 1.73	9.07 ± 1.11	14.5 ± 3.89	12.9 ± 2.33	12.39 ± 2.82
ESM MCs	8.31 ± 4.38	9.11 ± 2.30	7.85 ± 1.23	9.18 ± 2.81	8.11 ± 1.55

All MCs had a rough surface with interconnected porous surface structures (Fig. 2). Previous studies have indicated that rough surfaces are important to protect against shear stress and enhance cell attachment, and it is a common procedure to manipulate smooth MC surfaces to achieve a more complex structure [35]. Scanning electron microscopy (SEM) revealed distinct morphological features of the MCs (Fig. 2). Both collagen-based MCs were spherical with a sponge-like character and a diameter of approximately 2000 μm (Fig S1, Fig. 2A and B). The surface of collagen MCs appeared more even with a pore size of ~10–15 μm in diameter (Fig. 2C–D), while the hybrid MCs had deep folds and cavities with a thin collagen film covering the ESM particles (indicated by arrows) and pore sizes of ~2 μm in diameter (Fig. 2B–D). An optimal pore size may facilitate ROS and $^1O_2$ diffusion through the hybrid MCs and the presence of ESM could explain the higher reduction in primary amines. Considering the average myofiber is quite large, the pore size of the MCs might not facilitate sufficient space for myofiber formation. However, cell migration inside the MCs was not analyzed during this

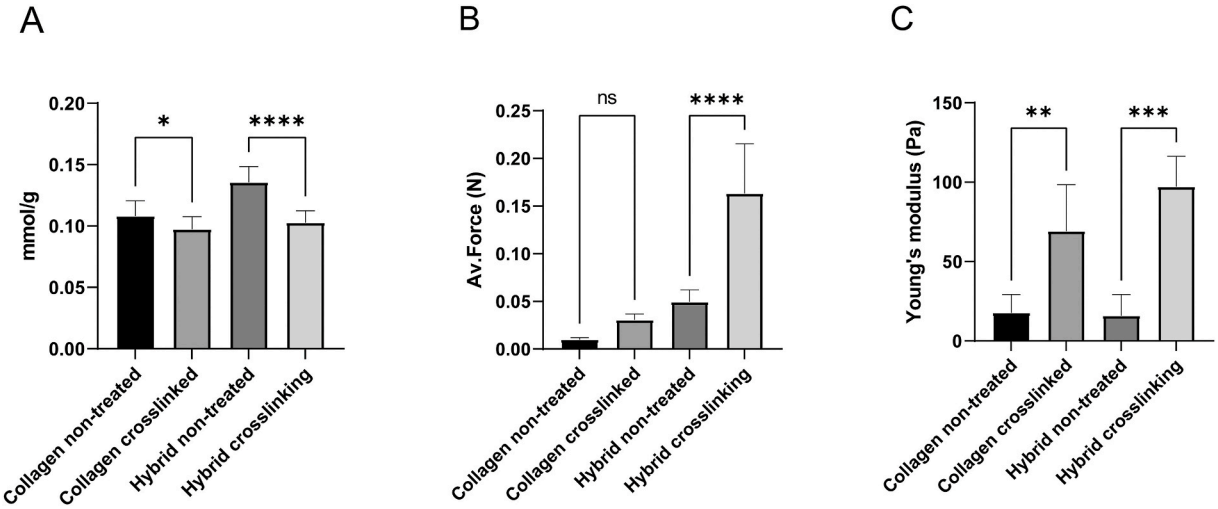

Fig. 1. Physical properties of collagen-based MCs. A) Content of primary amines mmol/g in the MCs were measured using TNBS-assay. Crosslinked MCs exhibited the lowest content of primary amines, indicating that the UVA-riboflavin treatment has successfully crosslinked the components in the MCs. B) The mechanical properties (force, N) of the derived collagen and hybrid MCs were measured using TA-XTplusC Texture Analyzer in compression mode. C) Elasticity of material (Young's modulus) defined as the slope of the stress-strain curve between 15 and 25% strain. Comparisons between non-treated and crosslinked for each MCs were analyzed using ordinary One-Way ANOVA with comparison between selected columns pairs, **p < 0.01, ***p < 0.0001***p < 0.0001).

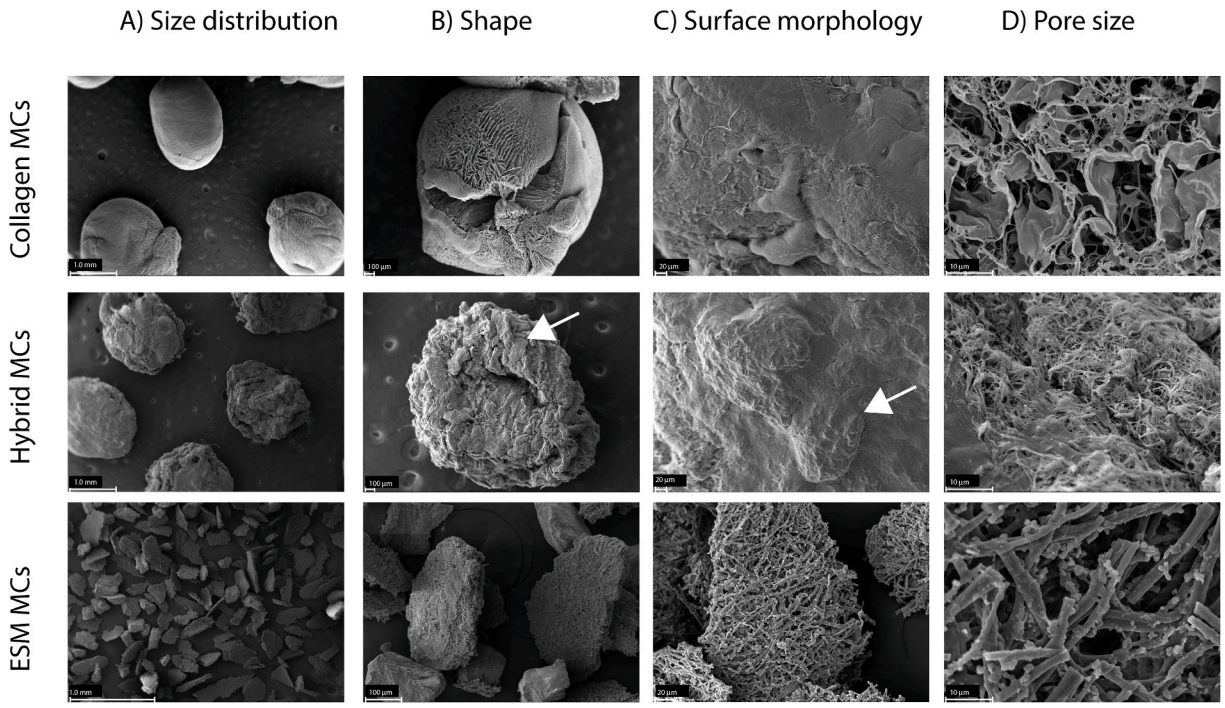

Fig. 2. Scanning electron microscope images showing A) size distribution, B) shape, C) surface morphology and D) pore size of the different MCs produced in this study. Representative pictures were selected from three different batches of each MC category. Arrows show ESM particle covered by a collagen film in the hybrid MCs. Scale bar is indicated with white lines.

work. In a study performed with human mesenchymal stem cells, the cells did not expand well on porous microcarriers, as compared with Cytodex®1 MCs [36]. Research has demonstrated that the freezing rate greatly determines the pore size of collagen-glycosaminoglycan (GAG) scaffolds, and the collagen-GAG suspensions frozen quickly in liquid nitrogen have smaller pores and irregular shapes [37–39]. Hence, it is possible to produce collagen MCs with larger pores and more uniform shapes by controlling the freezing temperature. While the ESM MC size was more comparable to the commercial Cytodex®1 MCs (Fig S1, 178 ± 25 μm and 261 ± 128 μm, respectively), the shape was different. SEM of ESM MCs showed tightly packed crosslinked fibers with an oval disk shape and a pore size diameter of 1–10 μm (Fig. 2, Fig S2). According to the manufacturer's report, Cytodex®1 MCs are solid spherical particles with ~190 μm diameter, made of dextran, and the surface is treated with positively charged diethylaminoethyl groups. While it is recognized that spherical particles provide good hydrodynamic properties and minimal stress on cells in agitated culture [4], the effects of shapes and sizes were not investigated in this study. Further investigation of the complete morphological parameters will be necessary after production optimization.

The appropriate size of a porous MC is essential. A smaller size means that a larger quantity of MCs can be suspended per liter culture medium, i.e., providing more surface area. Also, the MC interior can become nutrient-limited, and small MCs are easier to handle and analyze [4]. Therefore, reducing the size of the collagen-based MCs is an essential step for further optimization of MCs production. In this work, the technique used to produce collagen-based MCs depended on the solution density and interfacial tension because they were dripped into liquid nitrogen with a syringe. Other techniques can control the production process more efficiently while reducing the size of collagen-based MCs, such as wet spinning or custom-designed apparatus employing a droplet air-jet [23,40].

3.2. Skeletal muscle satellite cells successively attached to, spread, and proliferated on all MC types

The skeletal muscle satellite cell (MuSC) attachment and cell proliferation on the MCs were visualized by nuclear staining of live cells (Fig. 3). The observations showed that MuSCs successively attached and rapidly proliferated to cover the entire surface of all MC types, during the eight days of cell expansion. Agitation rate influence cell growth and high agitation rates (≥ 100 rpm) can inhibit cell growth. On the other hand, higher agitation rates might prevent aggregates [36]. In this work, no aggregation between MCs was observed with the 100 rpm agitation rate.

Because cells can sense the physiological conditions necessary for normal cellular behavior, the matrix surface properties are directly related to biological activity in vitro, such as cell attachment, spreading, and growth. When bovine MuSCs were expanded in spinner flasks, they formed cell-to-cell connections in monolayers, covering the entire surface of all the MCs (Fig. 4A–B). A more widespread morphology was observed on ESM and Cytodex®1 compared to collagen-based MCs (Fig. 4A–B). Biomaterials indented as scaffolds for cells to expand on can possess polypeptide motifs or ligands that promote a stronger and more rapid cell attachment and spreading through interaction with different cell adhesion signaling mechanisms. For example, the tri-amino acid sequence, arginine-glycine-aspartate (RGD), is a particularly widely studied adhesive peptide that acts as the principal integrin-binding domain present within ESM proteins [41]. It is well established that integrin receptors are the main cell adhesion molecules that regulate binding to ECM proteins such as collagen, fibronectin, and laminins. This is a crucial factor to consider for the successful development of biomaterials that retain cell-collagen binding motifs in tissue engineering and scaffolds [42]. The relative gene expression of integrin-subunit β5 (ITGβ5) was upregulated in MuSCs expanded on Cytodex®1 MCs, while the expression was dramatically increased on collagen and hybrid MCs (Fig. 4C). While using enzymes and acid is an effective technique to obtain high yield when extracting collagen, the method can interfere with cell-collagen interactions. These results clearly demonstrated that

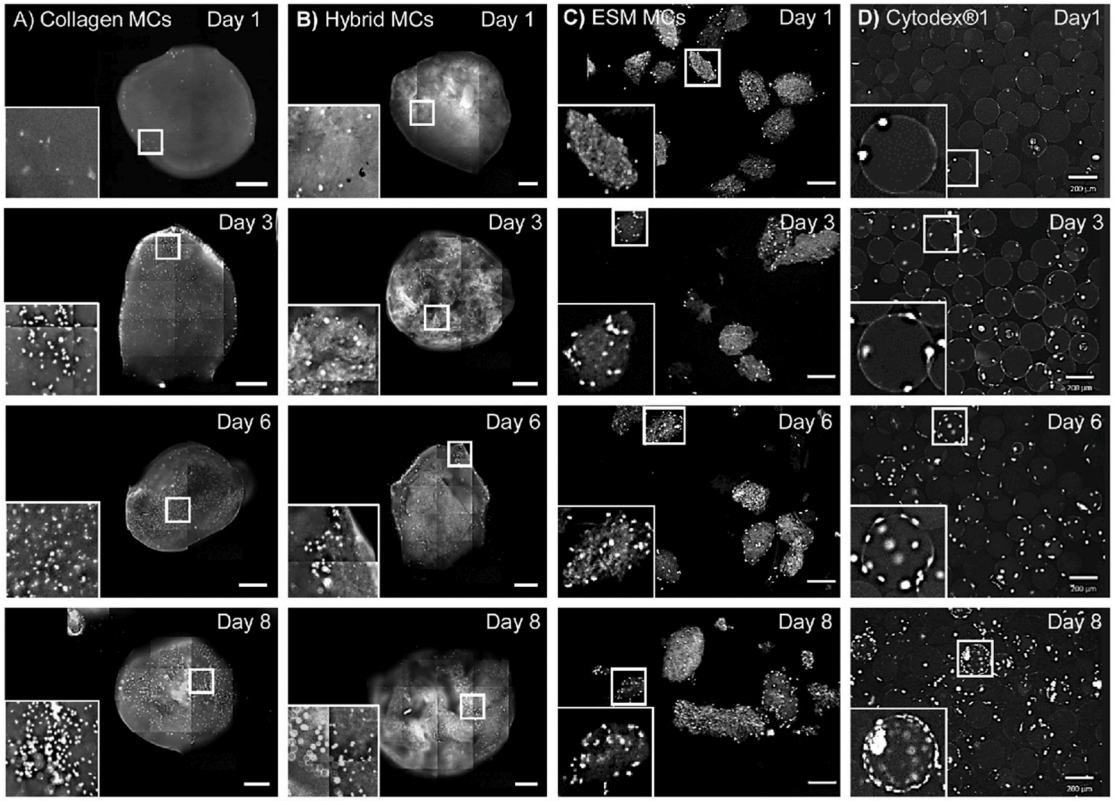

Fig. 3. Skeletal muscle satellite cell expansion over 8 days on MCs in spinner flask cell culture. Samples with collagen (A), hybrid (B), ESM(C) and Cytodex®1 (D) MCs were stained with NucBlue Live stain between day 1–8 and visualized with ZEISS Axio Observer Z1 microscope. Scale bars are indicated at 500 μm (A and B) and 200 μm (C and D). All MCs maintained their shape after prolonged cell culture. Representative pictures were selected from four different experiments, each with three replicate spinner flask experiments.

the molecular architecture of the turkey collagen used to generate MCs was suitable for cell adhesion, migration, and cell-collagen interaction through integrin receptors. Interestingly, the expression of ITGβ5 was reduced when cells were expanded on ESM MCs. Proteomics studies have identified structural proteins such as collagen and cysteine-rich eggshell membrane proteins (CREMPs) in processed ESM powder [22]. Therefore, we would expect similar cell interactions with this biomaterial as with collagen. However, our group has previously demonstrated that ESM powder can promote matrix metalloproteinase activity in human fibroblast cells, particularly MMP-9 and 2, which are involved in degrading collagen fibrils and therefore indirectly influences ITGβ5 expression [19].

Other receptor types can function as co-receptors for matrix proteins. It is demonstrated that syndecan-4 (*SDC4*) is a critical co-receptor. *SDC4* is necessary together with integrins for a complete adhesion-dependent signaling response. Also, *SDC4* is important for the assembly of focal adhesions (FA), mechanosensing, cell attachment, spreading, and can also act as the initial fibronectin sensor [43–46]. The importance of *SDC4* for normal skeletal muscle function has been illustrated by our and many other research groups [47–50]. Additionally, Karimi et al. reported that biomaterials engineered to display nanoclusters of ligands that bind both integrin and *SDC4* receptors increase cell adhesion of endothelial cells [51]. Relative gene expression of SDC4 was downregulated in MuSCs expanded on Cytodex®1 and upregulated when using collagen, hybrid, and ESM MCs (Fig. 4C). ESM has a complex structure containing collagen, fibronectin, fibrin, and vitronectin, in addition to a broad range of other glycoproteins and GAGs [18,43]. Therefore, the SDC4 upregulation observed when using ESM-containing MCs can partly be explained by the mechanical properties or complex mix of ECM constituents in ESM. This result is in line with the higher mechanical hardness of hybrid MCs than pure collagen MCs, where cells show a lower SDC4 expression [44]. Further, Vinculin (VCL) encodes a cytoplasmic actin-binding protein distributed throughout FA and mediates cell adhesion and migration. Previous reports have demonstrated that cell invasion into 3D collagen matrixes is regulated by VCL [52]. The expression of VCL followed the same pattern as ITGβ5, showing decreased expression in cells expanded on ESM MCs and upregulated expression in cells grown on collagen and Cytodex®1 MCs. In contrast, no change in expression was observed in MuSCs expanded on hybrid MCs. Altogether, our study demonstrated that MuSCs engage in specific interactions with the different by-product biomaterials. The different biomaterials may have opposing effects on the expression pattern of adhesion molecules. The surface chemistry of collagen and ESM modulated mRNA SDC4 upregulation in MuSCs. While collagen strongly induced ITGb5 and VCL expression upregulation, the ESM biomaterial modulated a downregulation in both genes, emphasizing the complexity of cell-matrix receptor signaling.

3.3. Skeletal muscle satellite cells retained their early myogenic and proliferation potential on all MC types

The relative gene expression of MKI67, a proliferation-associated factor increased over time in cells expanded on all MCs tested in this study, verifying that MuSCs were able to proliferate on all the MC types (Fig. 5A). Interestingly, the DNA concentration increased for all the food-grade MCs, however the cells seeded on Cytodex 1 MCs seemed to stop the growth after day 6 (Fig. 5B). The reason for this could be lack of available growth area, and a solution would be to add fresh MCs during the process to increase the area. The growth kinetics of the cells on Cytodex®1 MCs resembled the growth curves also obtained by Verbruggen et al. but the growth rate was slightly slower compared to the growth rate when cultured in conventional monolayer cultures [53,26].

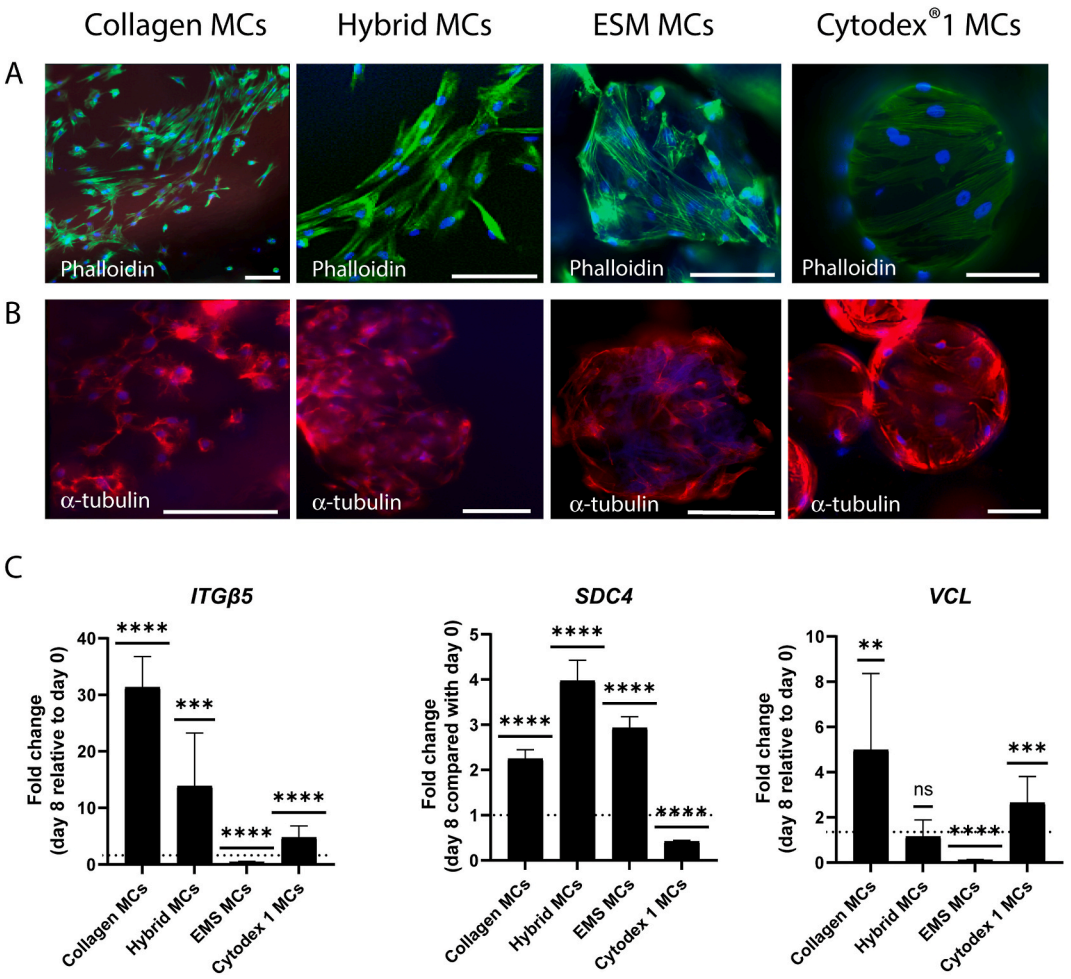

Fig. 4. Skeletal muscle satellite cell morphology and adhesion markers on different MCs in cell culture spinner flask systems after 8 days of expansion. Different components of the cytoskeleton, i.e., (A) F-Actin and (B) α-Tubulin were visualized with fluorescent immunostaining on collagen, hybrid, ESM and Cytodex®1 MCs. The cell nuclei were stained using the NucBlue Live stain (blue). Scale bars are indicated at 100 μm and the images were captured with ZEISS Axio Observer Z1 microscope. C) Relative gene expression of *SDC4*, *ITGb5* and *VCL* is presented as fold change at day 8 relative to mean day 0 (indicated with horizontal dotted line) within its own category, i.e., collagen, hybrid, ESM and Cytodex®1 MCs. The observations are represented as mean ± SD from at least three different experiments, each with three replicate spinner flasks experiments. Comparisons between day 8 versus day 0 for each type of MC were analyzed using one sample *t*-test with hypothetical value set to 1 (***p < 0.001, ****p < 0.0001). (For interpretation of the references to colour in this figure legend, the reader is referred to the Web version of this article.)

Next, we investigated the metabolic activity (glucose consumption and lactate production) of MuSCs during cell expansion. The observations showed that the MuSCs were metabolically active and viable on all the MCs (Fig. 6). This was demonstrated by a reduction in glucose concentration followed by an increase in lactate concentrations. Collagen-based MCs had the most considerable change in glucose and lactate concentrations, »-0.35 g/L and »+0.2 g/L, respectively. ESM and Cytodex®1 MCs had similar changes in glucose (»-0.2 g/L) and lactate (»+0.1 g/L) concentrations. These observations fit well with the dsDNA concentrations measured in the different cell cultures, indicating a higher cell proliferation on collagen-based MCs in spinner flasks than ESM and Cytodex®1 MCs. For all the MC types, we also observed a stable ATP production and low cytotoxicity (measured as release of LDH in the cell medium) over time (Fig. S3). Both collagens isolated from turkey and ESM powder are previously shown to stimulate cell growth of different cell types, including keratinocytes and dermal fibroblasts. The parameters discussed demonstrated the great cell growth-promotion potential and biocompatibility of these biomaterials with MuSCs.

The development of MuSCs is regulated by a series of transcription factors, such as paired boxed 7 (PAX7), which is highly expressed in quiescent and newly activated muscle satellite cells, and myogenic factor 5 (MYF5) and myoblast determination protein 1 (MYOD1) that are expressed in activated, proliferating, and early differentiating cells. Our results showed that the gene expression level of myogenic transcription factors differed in bovine MuSCs expanded on the various MC types in spinner flask cell culture. The relative gene expression of PAX7 decreased after eight days of expansion on all MCs relative to day 1 (Fig. 7A), and the expression was more reduced in cells expanded on ESM and Cytodex®1 compared to collagen and hybrid MCs. Further, the gene expression of MYF5 increased on all the MCs to similar levels (Fig. 7B). The transcriptome regulation, together with post-translational modifications, is complex. For example, considering that quiescent MuSCs have measurable mRNA levels of MYF5 and MYOD1, but due to post-transcriptional modifications these proteins are inhibited from translation into functional proteins until MuSCs are activated upon muscle damage [54]. This relationship is widely studied in human and mice cells [54–56]. Previous studies have demonstrated that MYF5 is directly regulated by PAX7 in mice myoblasts (C2C12) and that PAX7 is downregulated when cells are differentiated into myotubes [55]. However, other studies show that PAX7 is heterogeneously expressed in activated satellite cells, and 30% of satellite cells associated with freshly harvested myofibers from mice had undetectable levels of PAX7 [56].

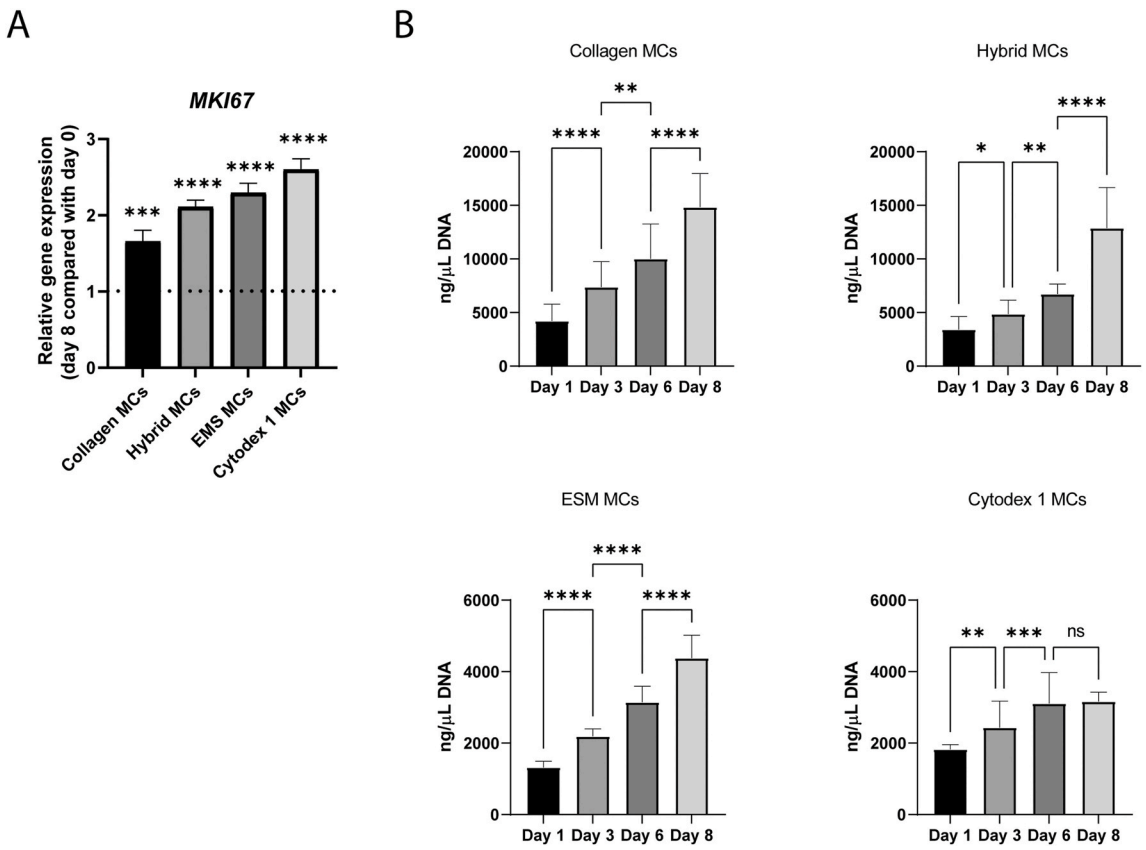

Fig. 5. Skeletal muscle satellite cell expansion on the different MCs for 8 days in spinner flasks. A) Relative gene expression (fold change) of proliferation marker *MKI67*. The data is presented as fold change at day 8 relative to mean day 0 (set to 1, indicated with horizontal dotted line) for each MCs i.e., collagen, hybrid, ESM and Cytodex®1. Comparisons between day 8 versus day 0 for each type of MC were analyzed using one sample *t*-test with hypothetical value set to 1 (***p < 0.001, ****p < 0.0001). B) Cell proliferation was expressed as the amount of dsDNA (ng/µl) at different time points. Outliers were identified and excluded using ROUT methods, with Q = 1%. Comparisons between the different time points for each MCs were analyzed using ordinary One-Way ANOVA with comparison between selected columns pairs (day 1-day 3, day 3-day 6, day 6-day 8. *p < 0.05, **p < 0.01, ***p < 0.001, ****p < 0.0001).

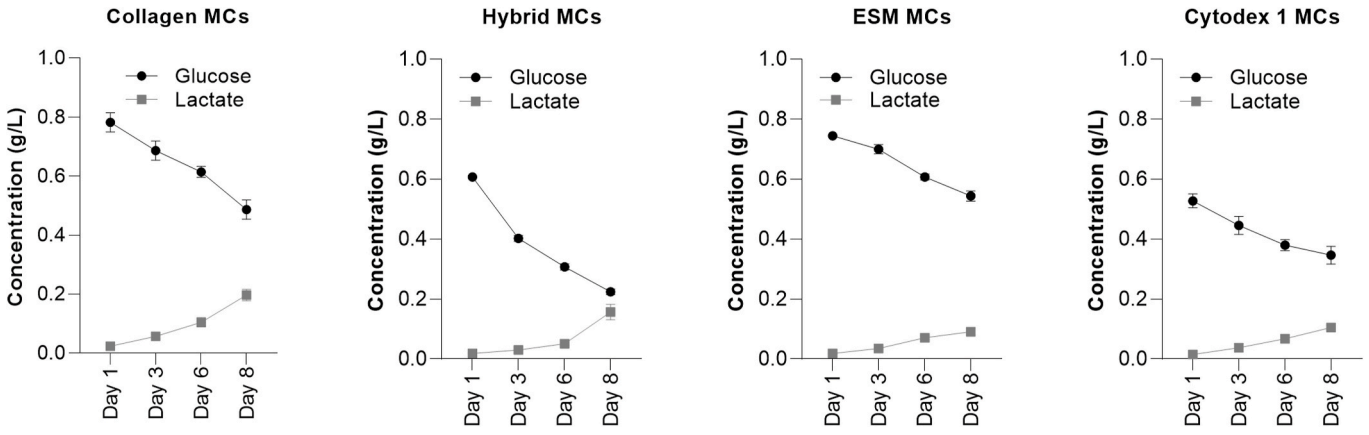

Fig. 6. Metabolic activity was measured as consumption of glucose and production of lactate. Data is presented as mean ± SD from at least three different experiments, each cell experiment using three replicate spinner flasks.

Further illustrating the complexity of the molecular mechanisms regulating myogenesis in MuSCs, and maybe especially across species. The cause of PAX7 down-regulation and MYF5 upregulation during cell expansion in these spinner flask experiments are unknown. However, Guo et al. describe evidence supporting using MYF5 to represent the muscle committed proliferating population because of the varying $PAX7^{+}MYF5^{-}$ to $PAX7^{+}MYF5^{+}$ cell proportions observed in cattle [57].

In contrast to PAX7 expressions, the mRNA expression of MYOD1 was increased in cells expanded on ESM and Cytodex®1 MCs, with the highest upregulation of MYOD1 on Cytodex®1. Interestingly the expression was reduced on the collagen-based MCs (Fig. 7). This is possibly due to the proliferation-stimulating effect in bovine cells observed with ESM MCs alone demonstrated by the mRNA expression of MYF5 and MKI67 (Figs. 7 and 5A). We have previously shown that surface coating greatly affected the proliferation of MuSCs. A complex extracellular matrix coating containing fibrous proteins like collagens

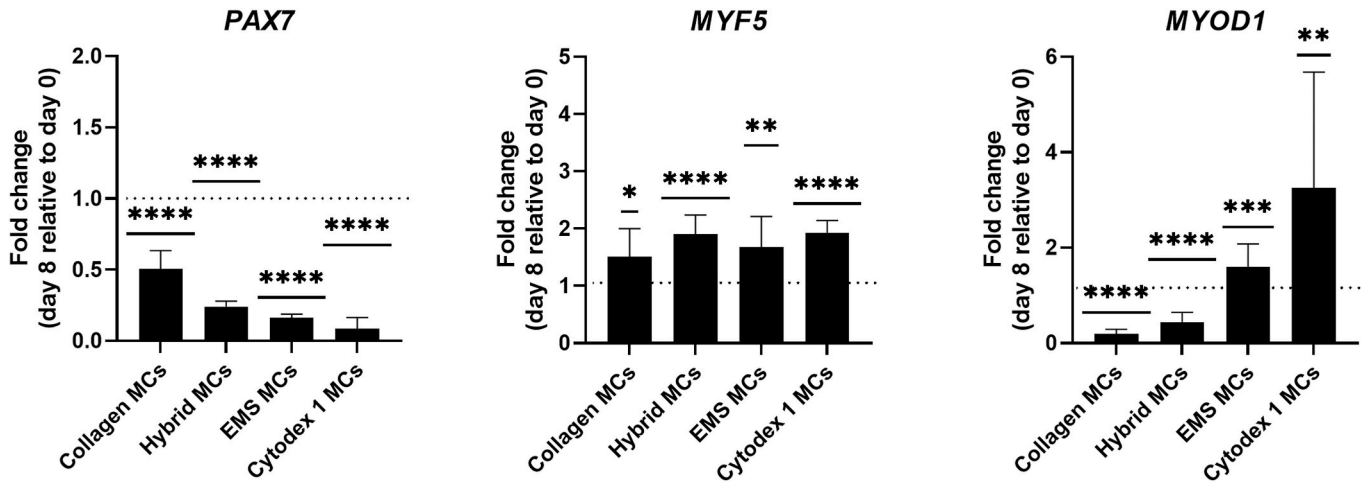

Fig. 7. Relative gene expression of transcription factors *PAX7*, *MYF5* and *MYOD1* during skeletal muscle satellite cell expansion on MCs in spinner flasks. The data is presented as fold change at day 8 relative to day 0 (set to 1, indicated with horizontal dotted line) within its MC category, i.e., collagen, hybrid, ESM and Cytodex®1. The bars are represented as mean ± SD from at least three different experiments, each with three replicate spinner flasks. Comparisons between day 8 versus day 0 for each type of MC were analyzed using one sample *t*-test with hypothetical value set to 1 (*p < 0.05, **p < 0.01, ***p < 0.001, ****p < 0.0001).

and GAGs greatly improved cell proliferation and early differentiation of MuSCs in 2D cell culture [26]. Together, these results indicate that although the MuSCs proliferated on all the MCs after eight days in spinner flasks, the MuSCs expression of myogenic transcription factors differed with the various MCs. The MuSCs expanded on collagen-based MCs, preserved their stem cell characteristics, and postponed differentiation initiation to a greater extent than cells grown on ESM and Cytodex®1 MCs. Immunostaining of the MuSCs specific marker CD56/NCAM on the different collagen-based MCs and eggshell membrane, demonstrated that cells interacting with these biomaterials express the marker after 8 days of cell culturing (Fig S4). NCAM was the first marker used to identify human muscle satellite cells, and this marker is expressed in satellite cells, myoblasts, myotubes and muscle fibers during development [58]. We have previously demonstrated this as specific MuSC marker for cells of bovine origin [26]. This marker is expressed in proliferating human and rat muscle cells but is not a reliable marker in mice muscle cells; mice muscle cells express NCAM only when they have become committed to differentiation [59]. Finally, we have previously performed immunostaining of CD56 together with mRNA MYOD1 analysis of bovine skeletal muscle cultured on larger collagen and ESM biomaterial scaffolds verifying that mRNA MYOD expressing bovine primary skeletal muscle cells express skeletal muscle myoblast protein markers on these biomaterials [21].

In this study, we used highly assessable biomaterial mimicking the structural and the complexity of ECM. According to a report presented by Lindberg et al. there were 7000 tons of by-products available from commercial turkey production, just in Norway in 2015. From chicken, nearly 22 000 tons of chicken by-products were available in 2015. Also, more than 40 tons of ESM are being produced annually [60]. Collagen extracted from turkey tendon, with its high denaturation temperature compared to collagen extracted from other species, restores fibrillar properties after extraction [16]. This material had good mechanical properties and high biocompatibility. This in contrast to gelatin, which is partially degraded and often is used to produce scaffolds and MCs [61]. ESM offer an interesting and naturally occurring materials that are largely considered as a waste product in the food industry. The ESM is a highly complex structured biomaterial consisting of collagens, glycoproteins and glycosaminoglycans [20] mimicking ECM complexity even further. This highly crosslinked biomaterial reduces the crosslinking step in the production of MCs which is often necessary for stabilization of the biopolymers. The commercial Cytodex®1 MCs used in the study consist of edible dextran biopolymers that has to be chemically crosslinked with RGD-sequences to allow cells to attach and proliferate. Cytodex®1 MCs are therefore not food-grade in an in vitro meat perspective. Both collagen, ESM as well as gelatin contains natural RGD-sequences, reducing the extra RGD-linker step [8]. To the best of our knowledge, few studies exist on food-grade MCs produced by assessable biomaterials from the industry for tested in agitated culture conditions. Liu and co-workers produced MCs based on egg-white, using an emulsifying strategy, however these were designed for use in biomedicine for drug delivery [62]. Other studies, using food-grade biomaterials have not been tested in agitated cell culturing systems, rather as static conditions as scaffolds [10,63]. Interesting studies exist as edible textured soy protein scaffold in static culture for bovine skeletal muscle expansion tested, and could also be a promising candidate for production of MCs [9].

4. Conclusions

We report that by-product biomaterials, with minimal processing, can function as MCs for culturing bovine MuSCs in spinner flask culture. We have produced three interconnected and porous MCs during this work, using entirely food-grade, low-cost, and biocompatible biomaterials, namely, turkey collagen and ESM. We showed that crosslinking collagen with UVA-riboflavin treatment improved resilience to degradation in agitated cell culture. Furthermore, the inclusion of ESM in collagen-based MCs increased the MCs' surface area and mechanical hardness. Bovine MuSCs successfully attached and covered all the different MCs' entire surfaces while demonstrating high cell proliferation and metabolic activity combined with low cytotoxicity. Further, relative gene expression of skeletal muscle markers (*PAX7, MYF5*) and proliferation marker *MKI67* indicated that MuSCs retained their early myogenic potential and proliferation capacity on the different MCs. Finally, mRNA expression of cell adhesion markers suggested that MuSCs had specific interactions with the various biomaterials. Altogether, our results demonstrated that these MCs have bioactive surfaces that can support high-density cell cultures. The findings consequently support our hypothesis that turkey collagen and ESM are excellent biomaterial prospects with great potential in the production of custom-fabricated food-grade MCs for bovine MuSCs. The raw materials used in the study are widely available, low-cost and food-grade. Further development and optimization of MCs based on turkey collagen and ESM can therefore be a vital step in making cultured meat production economically feasible.

Author contributions

R. Christel Andreassen: Data curation, formal analysis, methodology, writing-original draft, writing-review, and editing. Sissel Beate Rønning: Conceptualization, funding acquisition, supervision, visualization, writing-review, and editing. Nina Therese Solberg: Data curation, formal analysis, methodology, writing-review, and editing. Krister Gjestvang Grønlien: Data curation, formal analysis, methodology, writing-review, and editing. Vibeke Høst: Formal analysis. Kenneth Aase Kristoffersen: Data curation, formal analysis, methodology, writing-review, and editing Svein Olav Kolset: Methodology, writing-review, and editing. Mona Elisabeth Pedersen: Conceptualization, funding acquisition, project Administration, supervision, writing-review, and editing.

Declaration of competing interest

The authors declare that they have no known competing financial interests or personal relationships that could have appeared to influence the work reported in this paper.

Data availability

The raw/processed data required to reproduce these findings cannot be shared at this time due to technical or time limitations.

Acknowledgments

The Research Council of Norway is greatly acknowledged for the financial support through the projects “GrowPro” (no. 280381) and “Notably” (no. 280709). Funding from Norwegian Fund for Research Fees on Agricultural Products (“SusHealth” no. 314599 and “Precision”, no. 314111) is also acknowledged. We would like to thank Norilia AS for contribution with raw material by-product from turkey and ESM. The funding sources were not involved in planning, conducting, or writing this paper. We would like to thank Wilhelm Glomm, Senior Scientist at SINTEF INDUSTRY, for help with measuring porosity of the MCs, this is highly acknowledged.

Appendix A. Supplementary data

Supplementary data to this article can be found online at https://doi.org/10.1016/j.biomaterials.2022.121602.

References

[1] L. Melzener, K.E. Verzijden, A.J. Buijs, M.J. Post, J.E. Flack, Cultured beef: from small biopsy to substantial quantity, J. Sci. Food Agric. 101 (1) (2021) 7–14.
[2] M.J. Post, S. Levenberg, D.L. Kaplan, N. Genovese, J. Fu, C.J. Bryant, N. Negowetti, K. Verzijden, P. Moutsatsou, Scientific, sustainability and regulatory challenges of cultured meat, Nat. Food 1 (7) (2020) 403–415.
[3] R. Edmondson, J.J. Broglie, A.F. Adcock, L. Yang, Three-dimensional cell culture systems and their applications in drug discovery and cell-based biosensors, Assay Drug Dev. Technol. 12 (4) (2014) 207–218.
[4] F. Cahn, Biomaterials aspects of porous microcarriers for animal cell culture, Trends Biotechnol. 8 (5) (1990) 131–136.
[5] A.K.-L. Chen, X. Chen, A.B.H. Choo, S. Reuveny, S.K.W. Oh, Critical microcarrier properties affecting the expansion of undifferentiated human embryonic stem cells, Stem Cell Res. 7 (2) (2011) 97–111.
[6] H. Tavassoli, S.N. Alhosseini, A. Tay, P.P.Y. Chan, S.K. Weng Oh, M.E. Warkiani, Large-scale production of stem cells utilizing microcarriers: a biomaterials engineering perspective from academic research to commercialized products, Biomaterials 181 (2018) 333–346.
[7] S. Verbruggen, D. Luining, A. van Essen, M.J. Post, Bovine myoblast cell production in a microcarriers-based system, Cytotechnology 70 (2) (2018) 503–512.
[8] V. Bodiou, P. Moutsatsou, M.J. Post, Microcarriers for upscaling cultured meat production, Front. Nutr. 7 (2020) 10.
[9] T. Ben-Arye, Y. Shandalov, S. Ben-Shaul, S. Landau, Y. Zagury, I. Ianovici, N. Lavon, S. Levenberg, Textured soy protein scaffolds enable the generation of three-dimensional bovine skeletal muscle tissue for cell-based meat, Nat. Food 1 (4) (2020) 210–220.
[10] J. Enrione, J.J. Blaker, D.I. Brown, C.R. Weinstein-Oppenheimer, M. Pepczynska, Y. Olguín, E. Sánchez, C.A. Acevedo, Edible scaffolds based on non-mammalian biopolymers for myoblast growth, Materials 10 (12) (2017) 1404.
[11] A. Kornmuller, C.F.C. Brown, C. Yu, L.E. Flynn, Fabrication of extracellular matrix-derived foams and microcarriers as tissue-specific cell culture and delivery platforms, JoVE 122 (2017) 55436.
[12] A.D. Theocharis, S.S. Skandalis, C. Gialeli, N.K. Karamanos, Extracellular matrix structure, Adv. Drug Deliv. Rev. 97 (2016) 4–27.
[13] OECD, Food, A.O.o.t.U. Nations, OECD-FAO Agricultural Outlook 2021-2030, 2021.
[14] H. Jia, M. Hanate, W. Aw, H. Itoh, K. Saito, S. Kobayashi, S. Hachimura, S. Fukuda, M. Tomita, Y. Hasebe, H. Kato, Eggshell membrane powder ameliorates intestinal inflammation by facilitating the restitution of epithelial injury and alleviating microbial dysbiosis, Sci. Rep. 7 (2017) 43993.
[15] K.A. Kristoffersen, N.K. Afseth, U. Böcker, K. Riiser Dankel, M. Aksnes Rønningen, A. Lislelid, R. Ofstad, D. Lindberg, S.G. Wubshet, Post-enzymatic hydrolysis heat treatment as an essential unit operation for collagen solubilization from poultry by-products, Food Chem. (2022) 132201.
[16] K.G. Grønlien, M.E. Pedersen, K.W. Sanden, V. Høst, J. Karlsen, H.H. Tønnesen, Collagen from Turkey (Meleagris gallopavo) tendon: a promising sustainable biomaterial for pharmaceutical use, Sustain. Chem. Pharm. 13 (2019) 100166.
[17] J.N. Losso, M. Ogawa, Thermal stability of chicken Keel bone collagen, J. Food Biochem. 38 (3) (2014) 345–351.
[18] T.A. Ahmed, H.P. Suso, M.T. Hincke, In-depth comparative analysis of the chicken eggshell membrane proteome, J. Proteonomics 155 (2017) 49–62.
[19] T.T. Vuong, S.B. Rønning, T.A.E. Ahmed, K. Brathagen, V. Høst, M.T. Hincke, H. P. Suso, M.E. Pedersen, Processed eggshell membrane powder regulates cellular functions and increase MMP-activity important in early wound healing processes, PLoS One 13 (8) (2018), e0201975.
[20] T.T. Vuong, S.B. Rønning, H.P. Suso, R. Schmidt, K. Prydz, M. Lundström, A. Moen, M.E. Pedersen, The extracellular matrix of eggshell displays anti-inflammatory activities through NF-κB in LPS-triggered human immune cells, J. Inflamm. Res. 10 (2017) 83–96.
[21] S.B. Rønning, R.S. Berg, V. Høst, E. Veiseth-Kent, C.R. Wilhelmsen, E. Haugen, H. P. Suso, P. Barham, R. Schmidt, M.E. Pedersen, Processed eggshell membrane powder is a promising biomaterial for use in tissue engineering, Int. J. Mol. Sci. 21 (21) (2020).
[22] T.A.E. Ahmed, H.P. Suso, A. Maqbool, M.T. Hincke, Processed eggshell membrane powder: bioinspiration for an innovative wound healing product, Mater. Sci. Eng. C Mater. Biol. Appl. 95 (2019) 192–203.
[23] R. Tonndorf, E. Gossla, D. Aibibu, M. Lindner, M. Gelinsky, C. Cherif, Wet spinning and riboflavin crosslinking of collagen type I/III filaments, Biomed. Mater. 14 (1) (2018), 015007.
[24] N. Davidenko, C.F. Schuster, D.V. Bax, N. Raynal, R.W. Farndale, S.M. Best, R. E. Cameron, Control of crosslinking for tailoring collagen-based scaffolds stability and mechanics, Acta Biomater. 25 (2015) 131–142.
[25] S.G. Wubshet, D. Lindberg, E. Veiseth-Kent, K.A. Kristoffersen, U. Böcker, K.E. Washburn, N.K. Afseth, Chapter 8 - bioanalytical aspects in enzymatic protein hydrolysis of by-products, in: C.M. Galanakis (Ed.), Proteins: Sustainable Source, Processing and Applications, Academic Press2019, pp. 225-258.
[26] S.B. Rønning, M.E. Pedersen, P.V. Andersen, K. Hollung, The combination of glycosaminoglycans and fibrous proteins improves cell proliferation and early differentiation of bovine primary skeletal muscle cells, Differentiation 86 (1) (2013) 13–22.
[27] E. Veiseth-Kent, V. Høst, M.E. Pedersen, Preparation of proliferated bovine primary skeletal muscle cells for bottom-up proteomics by LC-MSMS analysis, in: S. B. Rønning (Ed.), Myogenesis: Methods and Protocols, Springer New York, New York, NY, 2019, pp. 255–266.
[28] S.A. Bustin, J.-F. Beaulieu, J. Huggett, R. Jaggi, F.S.B. Kibenge, P.A. Olsvik, L. C. Penning, S. Toegel, MIQE précis: practical implementation of minimum standard guidelines for fluorescence-based quantitative real-time PCR experiments, BMC Mol. Biol. 11 (1) (2010) 74.
[29] T.D. Schmittgen, K.J. Livak, Analyzing real-time PCR data by the comparative CT method, Nat. Protoc. 3 (6) (2008) 1101–1108.
[30] M.D. Shoulders, R.T. Raines, Collagen structure and stability, Annu. Rev. Biochem. 78 (1) (2009) 929–958.
[31] V.K. Kodali, S.A. Gannon, S. Paramasivam, S. Raje, T. Polenova, C. Thorpe, A novel disulfide-rich protein motif from avian eggshell membranes, PLoS One 6 (3) (2011), e18187.
[32] J. Du, M.T. Hincke, M. Rose-Martel, C. Hennequet-Antier, A. Brionne, L. A. Cogburn, Y. Nys, J. Gautron, Identifying specific proteins involved in eggshell membrane formation using gene expression analysis and bioinformatics, BMC Genom. 16 (2015) 792.
[33] R. Uemura, J. Miura, T. Ishimoto, K. Yagi, Y. Matsuda, M. Shimizu, T. Nakano, M. Hayashi, UVA-activated riboflavin promotes collagen crosslinking to prevent root caries, Sci. Rep. 9 (1) (2019) 1252.
[34] A.S. McCall, S. Kraft, H.F. Edelhauser, G.W. Kidder, R.R. Lundquist, H.E. Bradshaw, Z. Dedeic, M.J.C. Dionne, E.M. Clement, G.W. Conrad, Mechanisms of corneal tissue cross-linking in response to treatment with topical riboflavin and long-wavelength ultraviolet radiation (UVA), Investig. Ophthalmol. Vis. Sci. 51 (1) (2010) 129–138.
[35] Q. Zan, C. Wang, L. Dong, P. Cheng, J. Tian, Effect of surface roughness of chitosan-based microspheres on cell adhesion, Appl. Surf. Sci. 255 (2) (2008) 401–403.
[36] I. Takahashi, K. Sato, H. Mera, S. Wakitani, M. Takagi, Effects of agitation rate on aggregation during beads-to-beads subcultivation of microcarrier culture of human mesenchymal stem cells, Cytotechnology 69 (3) (2017) 503–509.

[37] C. Lloyd, J. Besse, S. Boyce, Controlled-rate freezing to regulate the structure of collagen-glycosaminoglycan scaffolds in engineered skin substitutes, J. Biomed. Mater. Res. B Appl. Biomater. 103 (4) (2015) 832–840.
[38] S.T. Boyce, D.J. Christianson, J.F. Hansbrough, Structure of a collagen-GAG dermal skin substitute optimized for cultured human epidermal keratinocytes, J. Biomed. Mater. Res. 22 (10) (1988) 939–957.
[39] N. Dagalakis, J. Flink, P. Stasikelis, J.F. Burke, I.V. Yannas, Design of an artificial skin. Part III. Control of pore structure, J. Biomed. Mater. Res. 14 (4) (1980) 511–528.
[40] A.E. Turner, L.E. Flynn, Design and characterization of tissue-specific extracellular matrix-derived microcarriers, Tissue Eng. C Methods 18 (3) (2012) 186–197.
[41] S.L. Bellis, Advantages of RGD peptides for directing cell association with biomaterials, Biomaterials 32 (18) (2011) 4205–4210.
[42] R. Parenteau-Bareil, R. Gauvin, F. Berthod, Collagen-based biomaterials for tissue engineering applications, Materials 3 (3) (2010) 1863–1887.
[43] S.A. Wilcox-Adelman, F. Denhez, P.F. Goetinck, Syndecan-4 modulates focal adhesion kinase phosphorylation, J. Biol. Chem. 277 (36) (2002) 32970–32977.
[44] R.M. Bellin, J.D. Kubicek, M.J. Frigault, A.J. Kamien, R.L. Steward Jr., H. M. Barnes, M.B. Digiacomo, L.J. Duncan, C.K. Edgerly, E.M. Morse, C.Y. Park, J. J. Fredberg, C.M. Cheng, P.R. LeDuc, Defining the role of syndecan-4 in mechanotransduction using surface-modification approaches, Proc. Natl. Acad. Sci. U. S. A. 106 (52) (2009) 22102–22107.
[45] M.D. Bass, K.A. Roach, M.R. Morgan, Z. Mostafavi-Pour, T. Schoen, T. Muramatsu, U. Mayer, C. Ballestrem, J.P. Spatz, M.J. Humphries, Syndecan-4-dependent Rac1 regulation determines directional migration in response to the extracellular matrix, J. Cell Biol. 177 (3) (2007) 527–538.
[46] F. Lin, X.D. Ren, G. Doris, R.A. Clark, Three-dimensional migration of human adult dermal fibroblasts from collagen lattices into fibrin/fibronectin gels requires syndecan-4 proteoglycan, J. Invest. Dermatol. 124 (5) (2005) 906–913.
[47] S.B. Rønning, C.R. Carlson, J.M. Aronsen, A. Pisconti, V. Høst, M. Lunde, K. H. Liland, I. Sjaastad, S.O. Kolset, G. Christensen, M.E. Pedersen, Syndecan-4(-/-) mice have smaller muscle fibers, increased Akt/mTOR/S6K1 and Notch/HES-1 pathways, and Alterations in extracellular matrix components, Front. Cell Dev. Biol. 8 (2020) 730.
[48] S.B. Rønning, C.R. Carlson, E. Stang, S.O. Kolset, K. Hollung, M.E. Pedersen, Syndecan-4 regulates muscle differentiation and is internalized from the plasma membrane during myogenesis, PLoS One 10 (6) (2015), e0129288.
[49] A. Keller-Pinter, K. Szabo, T. Kocsis, F. Deak, I. Ocsovszki, A. Zvara, L. Puskas, L. Szilak, L. Dux, Syndecan-4 influences mammalian myoblast proliferation by modulating myostatin signalling and G1/S transition, FEBS Lett. 592 (18) (2018) 3139–3151.
[50] S.G. Velleman, D.L. Clark, J.R. Tonniges, The effect of syndecan-4 and glypican-1 knockdown on the proliferation and differentiation of Turkey satellite cells differing in age and growth rates, Comp. Biochem. Physiol. Mol. Integr. Physiol. 223 (2018) 33–41.
[51] F. Karimi, V.J. Thombare, C.A. Hutton, A.J. O'Connor, G.G. Qiao, D.E. Heath, Beyond RGD; nanoclusters of syndecan- and integrin-binding ligands synergistically enhance cell/material interactions, Biomaterials 187 (2018) 81–92.
[52] C.T. Mierke, P. Kollmannsberger, D.P. Zitterbart, G. Diez, T.M. Koch, S. Marg, W. H. Ziegler, W.H. Goldmann, B. Fabry, Vinculin facilitates cell invasion into three-dimensional collagen matrices, J. Biol. Chem. 285 (17) (2010) 13121–13130.
[53] S. Verbruggen, D. Luining, A. van Essen, M.J. Post, Bovine myoblast cell production in a microcarriers-based system, Cytotechnology 70 (2) (2018) 503–512.
[54] J. Massenet, E. Gardner, B. Chazaud, F.J. Dilworth, Epigenetic regulation of satellite cell fate during skeletal muscle regeneration, Skeletal Muscle 11 (1) (2021) 4.
[55] I.W. McKinnell, J. Ishibashi, F. Le Grand, V.G. Punch, G.C. Addicks, J.F. Greenblatt, F.J. Dilworth, M.A. Rudnicki, Pax7 activates myogenic genes by recruitment of a histone methyltransferase complex, Nat. Cell Biol. 10 (1) (2008) 77–84.
[56] H.C. Olguin, B.B. Olwin, Pax-7 up-regulation inhibits myogenesis and cell cycle progression in satellite cells: a potential mechanism for self-renewal, Dev. Biol. 275 (2) (2004) 375–388.
[57] B. Guo, P.L. Greenwood, L.M. Cafe, G. Zhou, W. Zhang, B.P. Dalrymple, Transcriptome analysis of cattle muscle identifies potential markers for skeletal muscle growth rate and major cell types, BMC Genom. 16 (1) (2015) 177.
[58] L. Boldrin, F. Muntoni, J.E. Morgan, Are human and mouse satellite cells really the same? J. Histochem. Cytochem. 58 (11) (2010) 941–955.
[59] K.L. Capkovic, S. Stevenson, M.C. Johnson, J.J. Thelen, D.D. Cornelison, Neural cell adhesion molecule (NCAM) marks adult myogenic cells committed to differentiation, Exp. Cell Res. 314 (7) (2008) 1553–1565.
[60] D. Lindberg, K. Aaby, G.I.A. Borge, J.-E. Haugen, A. Nilsson, R. Rødbotten, S. Sahlstrøm, Kartlegging av restråstoff fra jordbruket, in: N. AS (Ed.), Nofima Rapport 67/2016, 2017.
[61] N. Orellana, E. Sánchez, D. Benavente, P. Prieto, J. Enrione, C.A. Acevedo, A New edible film to produce in vitro meat, Foods 9 (2) (2020).
[62] Y. Liu, Q. Huang, J. Wang, F. Fu, J. Ren, Y. Zhao, Microfluidic generation of egg-derived protein microcarriers for 3D cell culture and drug delivery, Sci. Bull. 62 (18) (2017) 1283–1290.
[63] J.D. Jones, A.S. Rebello, G.R. Gaudette, Decellularized spinach: an edible scaffold for laboratory-grown meat, Food Biosci. 41 (2021) 100986.